Bulletin of Glaciological Research 18 (2001) 1−8

Article

Response sensitivities of a summer-accumulation type glacier to climate changes indicated with a glacier fluctuation model

Nozomu NAITO[1], Yutaka AGETA[1], Masayoshi NAKAWO[1], Edwin D. WADDINGTON[2], Charles F. RAYMOND[2] and Howard CONWAY[2]

1 Institute for Hydrospheric-Atmospheric Sciences, Nagoya University, Nagoya 464-8601 JAPAN

2 Geophysics Program, University of Washington, Box 351650, Seattle, Washington 98195-1650 USA

(Received August 31, 2000 ; Revised manuscript received November 21, 2000)

Abstract

Sensitivities of a summer-accumulation type glacier in response to changes in air temperature and precipitation are investigated using a glacier fluctuation model. The model couples glacier dynamics to empirical mass balance equations obtained for a typical summer-accumulation type glacier in the eastern Nepal Himalayas. The geometry and seasonal variations in air temperature and precipitation are simplified in order to examine the principal characteristics of the sensitivities. The magnitude of the volume change and the volume response time are discussed and compared with those for a hypothetical winter-accumulation type glacier of equivalent geometry.

The volume change of a summer-accumulation type glacier is roughly twice as large in its magnitude for an air temperature change as for an equally probable precipitation change in east Nepal. Moreover, the volume response time of the glacier is shorter for the temperature change than for the precipitation change. Accordingly, we suggest that air temperature changes rather than precipitation changes are mainly responsible for the fluctuations of summer-accumulation type glaciers in east Nepal, as long as the likelihood of future shifts in air temperature and precipitation scale with their modern standard deviations. The summer-accumulation type glacier responds more quickly to a temperature change than does the winter-accumulation type glacier, and its magnitude of the volume response is smaller for a precipitation change than the winter-accumulation type glacier. There is a significant shortening of the response time for increasing magnitude of glacier shrinkage.

1. Introduction

Variations in mountain glaciers around the world are important in assessing the change in global sea level. Glaciers in the Asian highland regions, as well as in Alaska and Patagonia, are especially thought to make critical contributions to the sea level rise (Meier, 1984; Warrick *et al.*, 1996). Recent observations have shown many glaciers in the Himalayas to be retreating rapidly, and the Himalayan glaciers are considered to be vulnerable to the recent global warming (Nakawo *et al.*, 1997).

Most glaciers in the Asian highland regions, including the Himalayas, owe their accumulation mostly to summer snowfall during the Asian monsoon. The mass balance of summer-accumulation type glaciers is considered to be sensitive to changes in air temperature (e.g. Ageta, 1983; Fujita and Ageta, 2000). For example, an increase in air temperature will decrease the snow fraction of precipitation, thereby decreasing accumulation. It will also lower the surface albedo of a glacier, thereby increasing absorption of solar radiation and melting. The increase in air temperature itself will, moreover, increase the melting. Thus, warming has three negative effects on the mass balance of a summer-accumulation type glacier. In order to simulate glacier shrinkage in response to warming, however, it is necessary to consider glacier dynamics.

A set of empirical equations was obtained to evaluate glacier mass balance from air temperature and precipitation on Glacier AX010, a small debris-free glacier in east Nepal, by Ageta (1983), with revision by Ageta and Kadota (1992). By combining the empirical equations and a glacier dynamic model, Kadota *et al.* (1997) accurately simulated the recent record of shrinkage of Glacier AX010. Naito *et al.* (2000) also adapted the empirical equations through modification for the effects of supra-glacial debris in a glacier dynamic model, and successfully simulated the recent shrinkage of Khumbu Glacier, a large debris-covered glacier in east Nepal.

Here we use these same empirical equations to investigate the sensitivities of a summer-accumulation type glacier in response to changes in air temperature and precipitation. The geometry and seasonal variations in air temperature and precipitation are much simplified, and we compare the sensitivity of a summer-accumulation type glacier and a hypothetical winter-accumulation type glacier of equivalent geometry. We examine both the magnitude of glacier volume change and the volume response time.

2. Model description

2.1. *Basic scheme of the glacier fluctuation model*

We modeled a valley glacier on the bed of constant slope, the tangent of which was 0.2. Grid points were distributed with a horizontal spacing of 50 m, except near the glacier terminus, which is described later. Transverse cross sections at mid points between neighboring grid points divided the glacier into control-volumes (Patankar, 1980;

Lam and Dowdeswell, 1996). All transverse cross sections were assumed to be rectangular with a constant width of 500 m (Fig. 1).

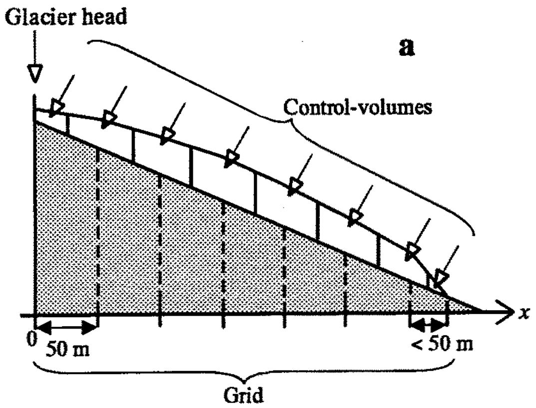

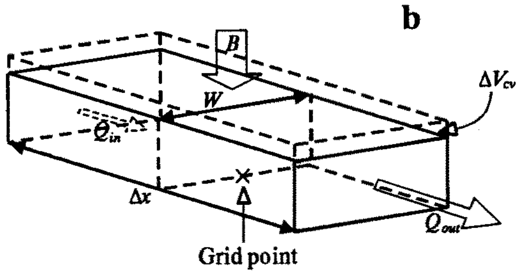

Fig. 1. (a) Longitudinal cross section of a glacier, illustrating the grid-system and control-volumes for simulation. (b) A projection of a control-volume, illustrating the continuity equation. Δx and W indicate the length and the width, respectively. ΔV_{cv}, B, Q_{in} and Q_{out} describe volume change, mass balance on the whole surface, and incoming and outgoing ice fluxes, respectively.

The fundamental equation for a glacier fluctuation model is the continuity equation for each control-volume:

$$\frac{\Delta V_{cv}}{\Delta t}=B-(Q_{out}-Q_{in}), \tag{1}$$

where ΔV_{cv} is volume change of a control-volume, B is mass balance on the surface of the control-volume, assuming no basal melting, and Q_{in} and Q_{out} are ice fluxes through the upper and lower boundary cross sections of the control-volume, respectively. The time interval was taken to be $\Delta t=1/36$ year (about 10 days). Setting x as a horizontal coordinate downstream along the central flow line,

$$B=bW\Delta x/\rho, \tag{2}$$

where b is mass balance in water equivalent at the central point of its surface, which is described in the following subsection, Δx and W (=500 m) are length and width of the control-volume, respectively, and $\rho=900$ kg m^{-3} is the density of ice.

An adaptive-grid system (Lam and Dowdeswell, 1996) was used to maintain smooth terminal fluctuations. Boundary conditions at the terminal grid point are zero ice thickness and zero outgoing flux (Q_{out}). Supposing a wedge-shaped terminal control-volume, its length (Δx) is not constant, but depends on its volume and ice thickness at the boundary cross-section with the neighboring upstream control-volume. If the distance between the terminal and the adjacent grid points exceeds the normal grid spacing (50 m), a new grid point is inserted. On the other hand, if the terminal control-volume disappears, the number of grid points decreases and the adjacent upstream control-volume is converted into a wedge-shaped terminal control-volume. Thus, the position of the terminal grid point varies smoothly. The two terminal control-volumes are re-divided at every time step by a new mid transverse cross-section between their grid points to conserve their total volume. As a result, the lengths of the terminal and the adjacent control-volumes vary from 0 to 25 m and from 25 to 50 m, respectively. The lengths of the glacier head control-volume and all the other control-volumes are constant at 25 m and 50 m, respectively, as illustrated in Fig. 1(a). The boundary condition at the glacier head grid point is zero incoming flux, but the ice thickness at the head grid point is not always zero.

To simulate time-dependent glacier fluctuations, an implicit, Crank-Nicholson scheme was used to approximate Eq. (1) as

$$\frac{V_{cv}^{i+1}-V_{cv}^{i}}{\Delta t}=\frac{1}{2}\left(B^{i+1}+B^{i}\right)-\frac{1}{2}\left[\left(Q_{out}^{i+1}+Q_{out}^{i}\right)-\left(Q_{in}^{i+1}+Q_{in}^{i}\right)\right]. \tag{3}$$

Superscripts refer to time step in the simulation. The volume of a control-volume at the next time step, V_{cv}^{i+1} ($=V_{cv}^{i}+\Delta V_{cv}$), is initially predicted by Eq. (1), using an explicit time scheme. Using the predicted value of V_{cv}^{i+1} with the glacier geometry, a surface profile of the glacier is predicted, and B^{i+1} and Q^{i+1} are evaluated through Eq. (2) and equations described in the following subsections. The value of V_{cv}^{i+1} can then be corrected with Eq. (3). These correcting procedures are iterated until differences between the predicted and the corrected values of V_{cv}^{i+1} become small (within 0.1% for all control-volumes).

2.2. *Mass balance calculation*

The mass balance, b, is represented by the empirical relations given by Ageta (1983) and Ageta and Kadota (1992) between mass balance components and air temperature, T (°C), for Glacier AX010:

$$c=\begin{cases} p, & \text{if } T<-0.6 \\ p(0.85-0.24T), & \text{if } -0.6\leq T\leq 3.5 \\ 0, & \text{if } T>3.5 \end{cases} \tag{4}$$

$$a=\begin{cases} 0, & \text{if } T<-3.0 \\ -0.0001(T+3.0)^{3.2}, & \text{if } -3.0\leq T\leq 2.0 \\ -0.009T, & \text{if } T>2.0 \end{cases} \tag{5}$$

$$b=c+a, \tag{6}$$

where p, c, and a are precipitation, accumulation and ablation (m w.e. day^{-1}), respectively. Although these empirical relations were obtained from the data for only one summer season, 1978, the relations are assumed to be applicable for the whole year.

A sinusoidal seasonal variation in air temperature is assumed as shown in Fig. 2. For summer-accumulation type mass balance, the seasonal distribution of precipitation is also assumed to be sinusoidal and in phase with the air temperature, reaching zero precipitation in the coldest season. Meteorological observations on Glacier AX010 by

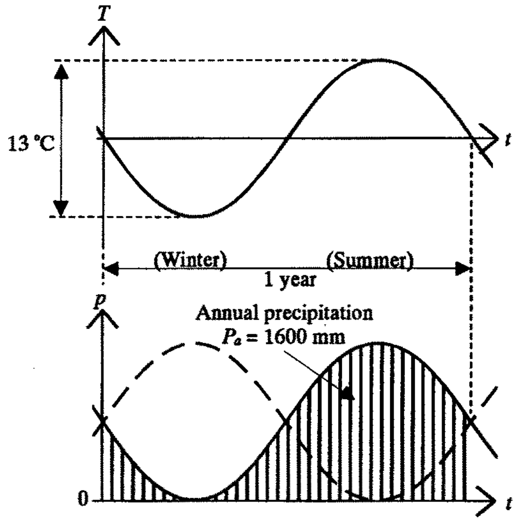

Fig. 2. Seasonal variation in air temperature and seasonal distribution of precipitation, assumed in this study. Both are simplified with sinusoidal variations. Distribution of precipitation on a summer-accumulation type glacier is set to be in phase with the temperature variation, and that on a winter-accumulation type glacier, indicated by the dashed line in the lower figure, is defined with a lag of 6 months behind that on the summer-accumulation type.

Ageta (1983) and Ageta *et al.* (1980) are used to estimate the climate. We assume an altitudinal lapse rate of $\Gamma=-6$°C km^{-1} and an annual range in air temperature of 13°C. The annual mean air temperature at the altitude of 4958 m is adjusted to -2.9°C, which leads to the mean temperature in the warmest four months of 2.4°C, as observed at the glacier terminus in 1978 by Ageta (1983). The annual precipitation is $P_a=1600$ mm, and it is assumed to be independent of altitude, as Ageta *et al.* (1980) observed for summer precipitation in 1978.

In order to evaluate the significance of the climate sensitivities, we compare the response of this hypothetical summer-accumulation type glacier with that of a hypothetical winter-accumulation type glacier exposed to a similar temperature cycle. The distribution of precipitation for the winter-accumulation type glacier has a lag of 6 months relative to the summer accumulation type, as shown in Fig. 2. Figure 3 shows the altitudinal profiles of annual mass balances and their components for both glacier types, calculated under the assumptions in this study. The difference in mass balance between the two types is due entirely to their difference in accumulation. The difference occurs because a larger proportion of precipitation falls as rain on the summer-accumulation type glacier. The difference becomes larger at lower altitudes due to higher air temperatures.

As illustrated in Fig. 3, the equilibrium line altitude (ELA) differs by 65 m between the two types. If the two type glaciers are simulated on the same bedrock, the accumulation area of the winter-accumulation type glacier would be larger and hence the winter-accumulation type glacier would be longer and bigger than the summer-accumulation type glacier. A large difference in the accumulation area would make it difficult to compare sensitivities of the two type glaciers. Therefore, bed altitude beneath the glacier head is adjusted to be 100 m higher than the corresponding ELA, which means that the bedrock is 65 m higher for the

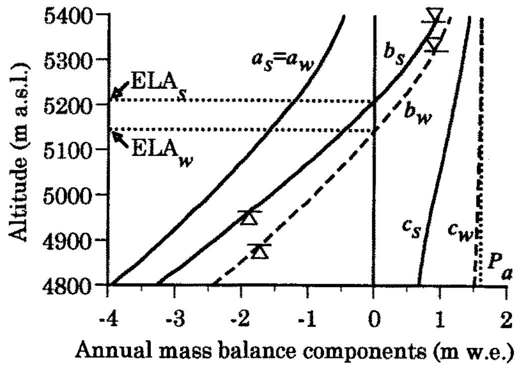

Fig. 3. Altitudinal profiles of annual mass balances and their components, calculated from Eq. (4)-(6) for the standard states in this study. The symbols, b, c, and a indicate annual amounts of mass balance, accumulation, and ablation, respectively. The subscripts, s and w, mean the values for the summer-(solid curves) and the winter-(dashed curves) accumulation types, respectively. Annual precipitation, P_a, is the same for both types and independent of altitude, as shown by the dotted line. The upper and lower horizontal bars with triangles for each type show the altitudes of the glacier head and terminus in the standard steady state, respectively, which are shown in Fig. 4.

summer-accumulation type glacier than for the winter-accumulation type glacier. The accumulation areas of the two type glaciers thus have almost the same surface area, although they are slightly different due to a difference in ice thickness around the ELA.

2.3. *Ice flux calculation*

Basal sliding is one of the most uncertain components in glacier dynamics. No direct measurement has been performed on basal sliding of glaciers in the Himalayas. Measurements of surface flow on Glacier AX010 showed no significant difference in the flow speed between summer and winter (Ikegami and Ageta, 1991); this suggests no basal sliding. Assuming no basal sliding, ice flux, Q, at the control-volume boundary is:

$$Q=f_2\frac{2A}{n+1}\left(-f_1\rho g\sin\alpha\right)^n H^{n+1}S \tag{7}$$

(Paterson, 1994, p. 334-335). Here, α, H and S are surface slope, ice thickness and transverse cross sectional area, respectively. The values of A and $n=3$ are parameters in the flow law of ice, f_1 is a factor accounting for lateral drag, f_2 is the ratio of the average speed through the cross-section to the central surface speed, and $g=9.81$ m s^{-2} is the acceleration due to gravity.

Measurements of ice temperature in glaciers in the Nepal Himalayas, e.g. Tanaka *et al.* (1980) on Glacier AX010 and Mae *et al.* (1975) on Khumbu Glacier, showed that the glaciers are not temperate. The ice temperature, however, is generally expected to be above -5°C. This study uses a constant value of $A=2.4\times10^{-15}$ s^{-1} kPa^{-3}, which corresponds to the recommended value for ice temperature of -2°C (Paterson, 1994, p. 97).

The so-called shape factor, f_1, is approximated by

$$f_1=1-\frac{0.30^{W/2H}+0.58^{W/2H}}{2}, \tag{8}$$

which is a regression for the values obtained by Nye (1965) for rectangular cross-sections. We use the flow speed ratio, $f_2=(n+1)/(n+2)=0.8$, for laminar flow in a very wide channel, which neglects transversal variations in flow.

3. Sensitivity experiments and their results

Starting from an initial ice-free condition, we ran the model until it reached a steady state for each type glacier, which we called a standard steady state. Here, a steady state was defined if the change in surface altitude from one year to the next was less than 0.1 m throughout the glacier. Longitudinal surface profiles of the standard steady states of the summer- and the winter-accumulation type glaciers are shown in Fig. 4. The surface altitude of each glacier head and the altitude of each glacier terminus are indicated in Fig. 3 by the upper and lower horizontal bars with triangles, respectively. Integration of mass balance from the head to the terminus along the longitudinal profile of the glacier surface was zero on each type glacier.

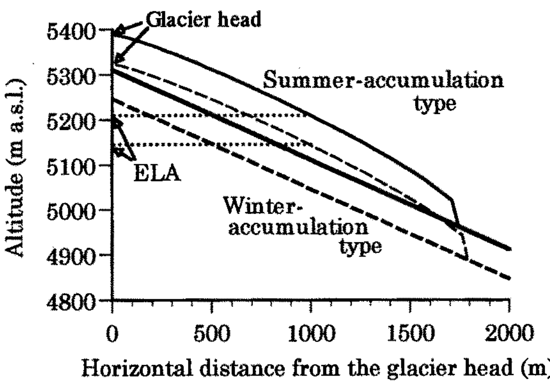

Fig. 4. Longitudinal profiles of the standard steady states for the summer- and the winter-accumulation type glaciers. Bed altitude beneath each glacier head is adjusted to 100 m higher than each ELA in the standard state, to equalize the extents of accumulation area for both types. Both glacier surface and bedrock are shown for the summer- and the winter-accumulation type glaciers by solid and dashed lines, respectively.

These standard steady states were the initial conditions for the following sensitivity experiments, in which air temperature was suddenly increased or precipitation was suddenly decreased. The sensitivity experiments ran until each glacier reached a new steady state. The perturbed ranges in temperature and precipitation were normalized with the equivalent standard deviations in annual records from 1971 to 1990 at Chialsa (DIHM, 1977, 1982, 1984, 1986; DHM, 1988, 1995): $\sigma_T=0.5$°C for annual mean air temperature and $\sigma_P=$ 267 mm ($=0.167P_a$) for annual precipitation. Here, the latter standard deviation for annual precipitation is based on the ratio of the standard deviation to the mean annual precipitation at Chialsa (319 mm/1914 mm=0.167). Chialsa is located at 2770 m a.s.l. in east Nepal about 20 km southeast of Glacier AX010 in the same drainage basin, and is the closest meteorological station to the glacier. We then repeated the experiments with different perturbations in temperature or precipitation, the magnitudes of which were changed by 0.1σ.

Figure 5 shows simulated variations in glacier volume, $V_{gl}(t)$, normalized by the volume at the standard steady state, $V_{gl}(0)$, following a perturbation of 1σ. Glacier volume

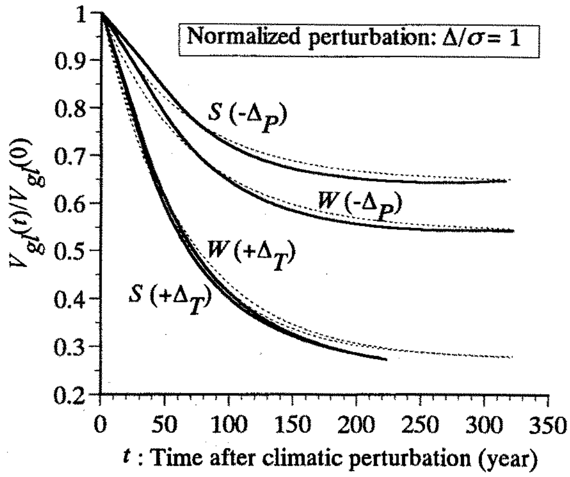

Fig. 5. Time dependent variations in normalized glacier volume, $V_{gl}(t)/V_{gl}(0)$, after a climatic perturbation of $\Delta=1\sigma$ (0.5°C or 267 mm). S and W mean the summer- and the winter-accumulation type glaciers, respectively, and $+\Delta_T$ ($=+0.5$°C) and $-\Delta_P$ ($=-267$ mm) indicate the cases for perturbation in air temperature and precipitation, respectively. The thick curves are simulated results, and the thin dotted curves are best fitting curves with Eq. (11).

appears to decrease exponentially to each new steady state; exponential curves that fit these responses are also shown by thin dotted curves in Fig. 5. The normalized total volume shrinkage to each new steady state, $\Delta V_{gl}(\infty)/V_{gl}(0)=1-V_{gl}(\infty)/V_{gl}(0)$, for the temperature perturbation is similar for the summer- and the winter-accumulation type glaciers. The volume shrinkage for the precipitation perturbation is, on the other hand, smaller for the summer-accumulation type than the winter-accumulation type. In addition, the volume shrinkage of each type glacier is larger for the temperature perturbation than for the precipitation perturbation. Figure 6 shows the normalized total volume shrinkage, $\Delta V_{gl}(\infty)/V_{gl}(0)$, for changing climatic (temperature or precipitation) perturbation normalized by the standard devi-

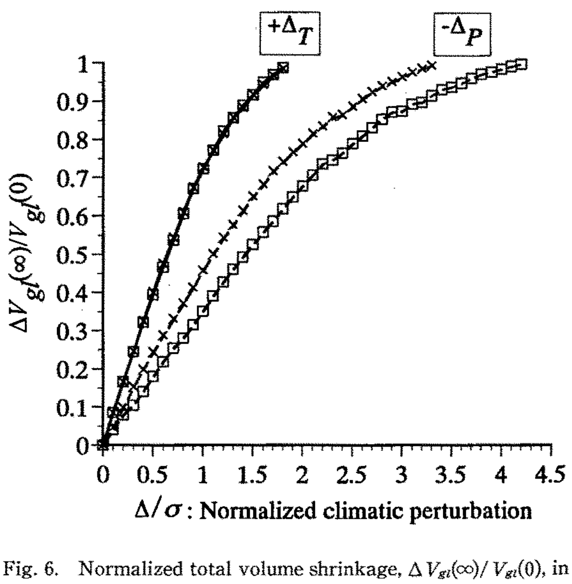

Fig. 6. Normalized total volume shrinkage, $\Delta V_{gl}(\infty)/V_{gl}(0)$, in response to changing climatic perturbations, Δ/σ, normalized by the modern standard deviation. Square and cross symbols represent the summer- and the winter-accumulation type glaciers, respectively. Solid and dashed curves indicate perturbations in air temperature and precipitation, respectively.

ation, Δ/σ. The features in $\Delta V_{gt}(\infty)/V_{gt}(0)$ are all the same for the whole range of the climatic perturbations as for $\Delta=1\sigma$ (Fig. 5). The magnitudes of the volume shrinkage for the temperature perturbations are similar for both type glaciers, while those for the precipitation perturbations are smaller for the summer-accumulation type glacier than the winter-accumulation type glacier. Those for the summer-accumulation type glacier are roughly twice as large for the temperature perturbations as for the precipitation perturbations. Moreover, Fig. 6 shows almost linear variations of $\Delta V_{gt}(\infty)/V_{gt}(0)$ to the climatic perturbations until $\Delta V_{gt}(\infty)/V_{gt}(0)$ reaches about 0.7, but the variations become non-linear for larger $\Delta V_{gt}(\infty)/V_{gt}(0)$.

4. Discussion

4.1. Magnitude of volume response

As shown in Fig. 6, the shrinkage of the summer-accumulation type glacier is roughly twice as large for a temperature perturbation as for an equally probable precipitation perturbation, judging from the standard deviations in records for the past 20 years at Chialsa. This suggests that the magnitude in fluctuations of summer-accumulation type glaciers in east Nepal would be controlled by changes in air temperature rather than in precipitation. Precipitation, however, can fluctuate largely depending upon the site. To obtain the same $\Delta V_{gt}(\infty)/V_{gt}(0)$ in case of the summer-accumulation type glacier in Fig. 6, the required normalized perturbation, Δ/σ, is 2 to 2.3 times as large for precipitation as for temperature. In other words, the volume shrinkage is larger for a temperature perturbation than for a precipitation perturbation if Δ_P/σ_P is not larger than $2\sim2.3\times\Delta_T/\sigma_T$. This conclusion, therefore, can hold as long as the ratio in the real fluctuating range in annual precipitation to annual air temperature, Δ_P/Δ_T, in east Nepal is not larger than $2\sim2.3\times\sigma_P/\sigma_T=1.1\sim1.2\times10^3$ mm °C^{-1}.

Figures 5 and 6 show that the magnitude of glacier shrinkage in response to warming is similar for both the summer- and the winter-accumulation types. As precipitation was assumed to be independent of altitude, raising temperature by Δ_T had equivalent meanings in the mass balance calculation to lowering altitude by a constant of Δ_T/Γ ; thereby the increase in ELA due to the warming was the same Δ_T/Γ for both glaciers. The glacier terminus in a steady state is located where the mass balance, integrated from the glacier head, reaches zero. As a result, the shrinkage due to warming is similar for both types. For the precipitation change, on the other hand, the magnitude of response is larger on the winter-accumulation type than the summer-accumulation type, as shown in Figs. 5 and 6. In this case, the precipitation change affected only accumulation, not ablation. Because the fraction of rainfall in precipitation is higher on the summer-accumulation type glacier, the same change in precipitation leads to less change in accumulation on the summer-accumulation type glacier.

It should be noted that the empirical Eq. (5), which was used to evaluate glacier ablation, implicitly includes the empirical albedo effect on ablation of Glacier AX010 with an exponent of 3.2 in the air temperature range between -3 and 2°C. This means that ablation is relatively suppressed at lower temperatures by the higher albedo of fresh snow cover and is relatively increased at higher temperatures by the lower albedo of a dirtier surface due to a decrease in the snowfall proportion (Ageta *et al.*, 1980). Because the winter-accumulation type glacier should have less fresh snow cover in the melting season than the summer-accumulation type, using Eq. (5) for the winter-accumulation type glacier should lead to overestimation of the suppressive effect of fresh snow on ablation, i.e., to underestimation of the ablation. As the underestimation of ablation should be severer at a lower temperature (higher altitude), the altitudinal gradients in ablation and mass balance of the winter-accumulation type should be smaller than those used in this model shown in Fig. 3. The increase in ablation on the winter-accumulation type glacier with a temperature increase, therefore, is overestimated in this model. Moreover, a decrease in precipitation should decrease the suppressive effect of fresh snow cover on ablation for the summer-accumulation type glacier. Thus, the ablation on the summer-accumulation type glacier should increase when precipitation decreases, although it was calculated independently of precipitation in this model. Further discussion on the differences in shrinkage magnitude between the two type glaciers in response to changes in air temperature and precipitation would require a more detailed model on the ablation process.

Setting $\Delta L_{gt}(\infty)/L_{gt}(0)$ and $\Delta H_{gt}(\infty)/H_{gt}(0)$ as the normalized decreases to each new steady state in the glacier length and the average glacier thickness, respectively,

$$1-\frac{\Delta V_{gt}(\infty)}{V_{gt}(0)}=\left(1-\frac{\Delta L_{gt}(\infty)}{L_{gt}(0)}\right)\left(1-\frac{\Delta H_{gt}(\infty)}{H_{gt}(0)}\right)$$

$$\frac{\Delta V_{gt}(\infty)}{V_{gt}(0)}=\frac{\Delta L_{gt}(\infty)}{L_{gt}(0)}+\frac{\Delta H_{gt}(\infty)}{H_{gt}(0)}-\frac{\Delta L_{gt}(\infty)}{L_{gt}(0)}\frac{\Delta H_{gt}(\infty)}{H_{gt}(0)}, \quad (9)$$

because the glacier width, W, is assumed to be constant. If both $\Delta L_{gt}(\infty)/L_{gt}(0)$ and $\Delta H_{gt}(\infty)/H_{gt}(0)$ vary linearly with the climatic perturbation, then, the variations in $\Delta V_{gt}(\infty)/V_{gt}(0)$ shown in Fig. 6 should be quadratic. Sensitivity experiments show that the variation in $\Delta L_{gt}(\infty)/L_{gt}(0)$ is almost linear with the climatic perturbation. On the other hand, the variation in $\Delta H_{gt}(\infty)/H_{gt}(0)$ is almost linear for large climatic perturbations, but approaches zero non-linearly for small climatic perturbations, as shown in Fig. 7. The subdued decrease in the average glacier thickness is due to a smaller

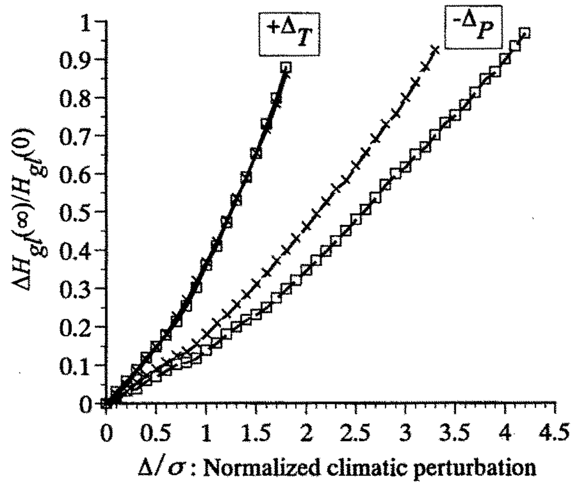

Fig. 7. Normalized decreases in average glacier thickness, $\Delta H_{gt}(\infty)/H_{gt}(0)$, in response to changing climatic perturbations, Δ/σ. The legends are the same as in Fig. 6.

altitudinal gradient of mass balance at a higher altitude, as shown in Fig. 3. The glacier thickness does not decrease as much on the upper part of the glacier for a small climatic perturbation as on the lower part. The variation of the glacier volume appears almost linear for small climatic perturbations in Fig. 6 as a result of the subdued decrease in the average glacier thickness. It then appears quadratic for large climatic perturbations due to the linear decreases in both the length and the average thickness of the glacier.

4.2. *Volume response time*

Besides the magnitude of the response described in the preceding subsection, a volume response time is introduced here to discuss the other factor in the sensitivity of glacier response to climate changes. Jōhannesson *et al.* (1989a, b) derived a theoretical estimate of a volume response time, τ_1, as:

$$\tau_1 = \frac{\langle H \rangle}{-b_t}, \tag{10}$$

where $\langle H \rangle$ means a characteristic thickness of the glacier, e.g. the maximum thickness, and b_t is the mass balance at its terminus, which is negative. The theoretical response time in the standard steady state was calculated to be 53 years for the summer-accumulation type glacier, which is shorter than that for the winter-accumulation type glacier of 59 years.

Mass balance conditions, however, vary according to surface altitude change as a function of time. The feedback between time-dependent surface altitude and mass balance makes the true volume response time somewhat longer than τ_1 (Jōhannesson *et al.*, 1989b; Jōhannesson, 1997; Harrison *et al.*, in press). A dynamic model simulation can take the feedback into account and represent the true response better than the simple response time, τ_1. As shown in Fig. 5, the volume change in response to a climatic perturbation can be approximated with an exponential curve:

$$\Delta V_{gl}(t) = V_{gl}(0) - V_{gl}(t) = \Delta V_{gl}(\infty)\left[1 - \exp\left(-\frac{t}{\tau_2}\right)\right], \tag{11}$$

where $\Delta V_{gl}(t)$ is the magnitude of the glacier volume change from the standard steady state at time t after a perturbation. A time constant, τ_2, which we define as a volume response time, is determined by finding the best match between Eq. (11) and the simulated volume change. Figure 8 shows the response time, τ_2, for a range of climatic perturbations, Δ/σ, and Fig. 9 shows τ_2 as a function of the normalized total volume shrinkage, $\Delta V_{gl}(\infty)/V_{gl}(0)$. Figures 8 and 9 do not include the cases of small climatic perturbations that lead to $\Delta V_{gl}(\infty)/V_{gl}(0)$ smaller than 0.3 because of the following model problem. A small oscillation in the transient glacier volume, which consists of an over-shrinkage and a rebound, can sometimes appear when the number of grid points changes or the glacier approaches its new steady state, even with an adaptive-grid system (Lam and Dowdeswell, 1996). The oscillations are usually negligible when the total volume changes are substantial, but hinder the determination of τ_2 (finding the best matching exponential curve to the simulated volume change) when the total volume changes are small.

The response time is shorter for temperature perturbations than for precipitation perturbations on both the summer- and the winter-accumulation type glaciers. In the preceding subsection we suggested that summer-accumulation type glaciers in east Nepal should be controlled by temperature changes rather than by precipitation changes; the shorter response times for temperature changes further support this idea. The response time, τ_2, is generally longer than the theoretical estimate, τ_1, as expected by Jōhannesson *et al.* (1989b), Jōhannesson (1997) and Harrison *et al.* (in press), except for relatively large perturbations.

In case of temperature perturbations, the summer-accumulation type glacier has a shorter response time than the winter-accumulation type glacier, as shown in Figs. 8 and 9. In the case of precipitation perturbations, on the other hand, the summer-accumulation type glacier has a response time similar to the winter-accumulation type glacier for Δ/σ smaller than 1.5 and a longer response time for Δ/σ larger than this, as shown in Fig. 8. These differences are likely to be due to difference in a shortening trend in the response time for large volume loss. According to Fig. 9, the summer-accumulation type glacier has a slightly longer response time than the winter-accumulation type glacier for precipitation perturbations that lead to the same normalized volume loss.

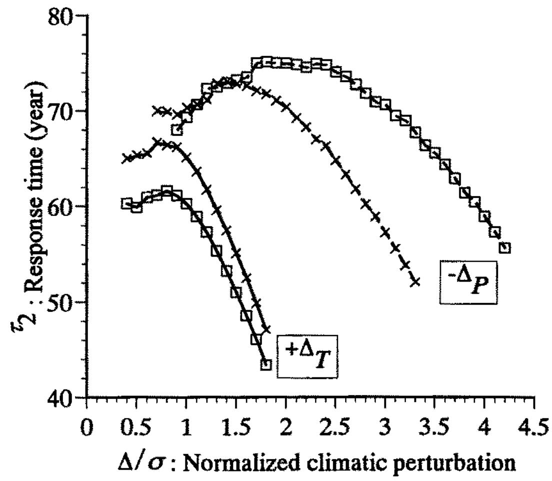

Fig. 8. Response time, τ_2, as a function of normalized climatic perturbation, Δ/σ, except the small perturbations that lead to $\Delta V_{gl}(\infty)/V_{gl}(0)$ smaller than 0.3. The legends are the same as in Fig. 6.

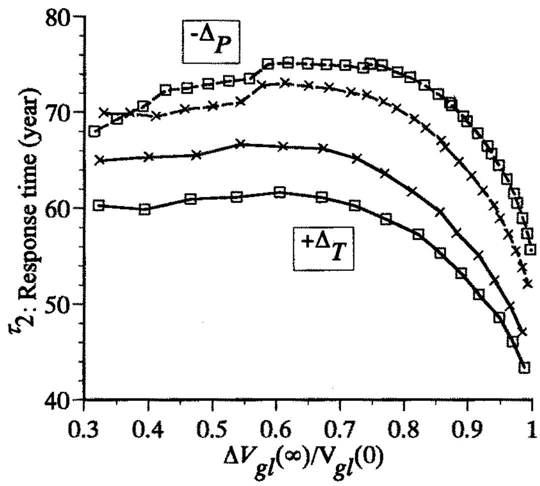

Fig. 9. Response time, τ_2, as a function of normalized total volume shrinkage, $\Delta V_{gl}(\infty)/V_{gl}(0)$, larger than 0.3. The legends are the same as in Fig. 6.

The response time seems to have a maximum around $\Delta V_{gl}(\infty)/V_{gl}(0)=0.6$ in Fig. 9, although the variation in response time is small around each maximum. Shortening of the response time is significant for $\Delta V_{gl}(\infty)/V_{gl}(0)$ larger than about 0.7 in Fig. 9. This indicates that the approach to a new steady state would be significantly faster for a climatic perturbation larger than that leading to $\Delta V_{gl}(\infty)/V_{gl}(0)=0.7$. In terms of the time scale of Jóhannesson *et al.* (1989a, b) given by Eq. (10), this shortening trend in the response time for large climatic perturbations could be attributed to the reduced effective glacier thickness as the glaciers shrink. The disappearance of the trend for small climatic perturbations might be due to the relatively subdued decrease in the glacier thickness, shown in Fig. 7. It is interesting to further examine the variation in the response time for climatic changes, including the glacier growth cases.

An actual glacier has an individual geometry and areal distribution in altitude, and a large glacier in the Himalayas usually has a complex mass balance pattern on its debris-covered area. This study neglected these complexities, and focused on sensitivity experiments to clarify the principal characteristics of an idealized summer-accumulation type glacier in response to climate changes. To forecast actual glacier fluctuations in the Himalayas, more realistic glacier geometry and scenarios for climate change would be desired, e.g. gradual warming rather than the sudden perturbation, and coupled changes in temperature and precipitation (Oerlemans *et al.*, 1998).

5. Concluding remarks

The principal characteristics of a summer-accumulation type glacier in response to air temperature and precipitation change were investigated by sensitivity experiments with a numerical model coupling both glacier dynamics and mass balance. We investigated both the magnitude of the volume change and the volume response time. The volume shrinkage of a summer-accumulation type glacier was roughly twice as large for an increase in air temperature compared to an equally probable decrease in precipitation, based on the standard deviations in recent meteorological records at Chialsa, east Nepal. The volume response time of the summer-accumulation type glacier was shorter for the temperature change than for the equally probable precipitation change. Accordingly, we suggested that changes in air temperature rather than in precipitation control fluctuations of summer-accumulation type glaciers in east Nepal as long as the range of changes in temperature and precipitation do not differ much from their modern standard deviations in the region. A summer-accumulation type glacier should then respond more rapidly to changes in air temperature and should have a smaller magnitude of volume change when responding to changes in precipitation, compared with an equivalent winter-accumulation type glacier. A significant shortening trend in the response time was shown for large climatic changes that lead to volume losses larger than 70% of the standard steady state.

Acknowledgments

This study was supported by Cooperative Research under the Japan-US Cooperative Science Program from the Japan Society for the Promotion of Science; US National Science Foundation Grant No. INT-9726704 from the National Science Foundation, USA; and a Grant-in-Aid for Scientific Research (Project No. 09490018) from the Ministry of Education, Science, Sports and Culture of Japan.

References

Ageta, Y. (1983): Characteristics of mass balance of the summer-accumulation type glacier in the Nepal Himalaya. Seppyo, **45**(2), 81-105. [In Japanese with English abstract.]

Ageta, Y. and Kadota, T. (1992): Predictions of changes of glacier mass balance in the Nepal Himalaya and Tibetan Plateau: a case study of air temperature increase for three glaciers. Ann. Glaciol., **16**, 89-94.

Ageta, Y., Ohata, T., Tanaka, Y., Ikegami, K. and Higuchi, K. (1980): Mass balance of Glacier AX010 in Shorong Himal, East Nepal during the summer monsoon season. Seppyo, **41**, Special Issue, 34-41.

Department of Hydrology and Meteorology (1988; 1995): Climatological Records of Nepal 1985-1986; 1987-1990. Ministry of Water Resources, Nepal, Kathmandu, 232pp.; 519pp.

Department of Irrigation, Hydrology and Meteorology (1977): Climatological Records of Nepal 1971-1975 Volume I. Ministry of Food, Agriculture and Irrigation, Nepal, Kathmandu, 366pp.

Department of Irrigation, Hydrology and Meteorology (1982; 1984; 1986): Climatological Records of Nepal 1976-1980; 1981-1982; 1983-1984 Volume I. Ministry of Water Resources, Nepal, Kathmandu, 410pp.; 174pp.; 187pp.

Fujita, K. and Ageta, Y. (2000): Effect of summer accumulation on glacier mass balance on the Tibetan Plateau revealed by mass-balance model. J. Glaciol., **46**, 244-252.

Harrison, W. D., Elsberg, D. H., Echelmeyer, K. A. and Krimmel, R. M. (in press): On the characterization of glacier response by a simple time constant. J. Glaciol., in press.

Ikegami, K. and Ageta, Y. (1991): Ice flow of Glacier AX010 in the Nepal Himalayas. Bull. Glacier Res., **9**, 17-22.

Jóhannesson, T. (1997): The response of two Icelandic glaciers to climatic warming computed with a degree-day glacier mass-balance model coupled to a dynamic glacier model. J. Glaciol., **43**, 321-327.

Jóhannesson, T., Raymond, C. F. and Waddington, E. D. (1989a): A simple method for determining the response time of glaciers. In Glacier Fluctuations and Climate Change. ed. by Oerlemans, J., Kluwer Academic Publishers, Dordrecht, 343-352.

Jóhannesson, T., Raymond, C. F. and Waddington, E. D. (1989b): Time-scale adjustment of glaciers to changes in mass balance. J. Glaciol., **35**, 355-369.

Kadota, T., Fujita, K., Seko, K., Kayastha, R. B. and Ageta, Y. (1997): Monitoring and prediction of shrinkage of a small glacier in the Nepal Himalaya. Ann. Glaciol., **24**, 90-94.

Lam, J. K.-W. and Dowdeswell, J. A. (1996): An adaptive-grid finite-volume model of glacier-terminus fluctuations. Ann. Glaciol., **23**, 86-93.

Mae, S., Wushiki, H., Ageta, Y. and Higuchi, K. (1975): Thermal drilling and temperature measurements in Khumbu Glacier, Nepal Himalayas. Seppyo, **37**, 161-169.

Meier, M. F. (1984): Contribution of small glaciers to global sea level. Science, **226**, 1418-1421.

Naito, N., Nakawo, M., Kadota, T. and Raymond, C. F. (2000): Numerical simulation of recent shrinkage of Khumbu Glacier, Nepal Himalayas. In Debris-Covered Glaciers (Proceedings of a workshop held at Seattle, Sep. 2000). ed. by Nakawo, M., Raymond, C. F. and Fountain, A., IAHS Publication no. 264, 245-254.

Nakawo, M., Fujita, K., Ageta, Y., Shankar, K., Pokhrel, A. P. and Yao T. (1997): Basic studies for assessing the impacts of the global warming on the Himalayan cryosphere, 1994-1996. Bull. Glacier Res., **15**, 53-58.

Nye, J. F. (1965): The flow of a glacier in a channel of rectangular, elliptic or parabolic cross-section. J. Glaciol., **5**, 661-690.

Oerlemans, J., Anderson, B., Hubbard, A., Huybrechts, P., Jóhannesson, T., Knap, W. H., Schmeits, M., Stroeven, A. P., van de Wal, R. S. W., Wallinga, J. and Zuo, Z. (1998): Modelling the response of glaciers to climate warming. Climate Dynamics, **14**, 267-274.

Patankar, S. V. (1980): Numerical Heat Transfer and Fluid Flow. Hemisphere, New York, 197pp.
Paterson, W. S. B. (1994): The Physics of Glaciers. Third Edition. Elsevier Science Ltd., Oxford, 480pp.
Tanaka, Y., Ageta, Y. and Higuchi, K. (1980): Ice temperature near the surface of Glacier AX010 in Shorong Himal, East Nepal. Seppyo, **41**, Special Issue, 55-61.
Warrick, R. A., Le Provost, C., Meier, M. F., Oerlemans, J. and Woodworth, P. L. (1996): Changes in sea level. In Climate Change 1995, the Science of Climate Change. ed. by Houghton, J. T., Meira Filho, L. G., Callander, B. A., Harris, N., Kattenberg, A. and Maskell, K., Cambridge University Press, Cambridge, 363-405.